Future Medicine Ltd
Immunotherapy
Volume 14, Issue 18, December 2022, Pages 1467-1480
https://doi.org/10.2217/imt-2022-0121

Research Article

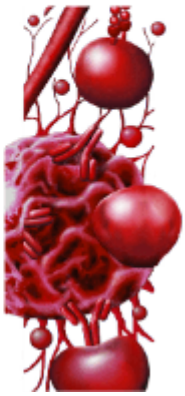

Antigen-independent tumor targeting by CBX-12 (alphalex™–exatecan) induces long-term antitumor immunity

Sophia Gayle [1], Timothy Paradis [1], Kelli Jones [1], Juan Vasquez [2] & Vishwas M Paralkar [1,*]

[1] Cybrexa Therapeutics, New Haven, CT 06511, USA

[2] Section of Hematology & Oncology, Department of Pediatrics, Yale University School of Medicine, New Haven, CT 06520, USA

[*] Author for correspondence: vishwas.paralkar@cybrexa.com

Aims: To determine whether antigen-independent targeting of the TOP1 inhibitor exatecan to tumor with a pH-sensitive peptide (CBX-12) produces superior synergy with immunotherapy compared with unconjugated exatecan. **Materials & methods:** *In vitro* and *ex vivo* functional assays were performed via FACS and ELISA assays. *In vivo* efficacy was evaluated in the syngeneic CT26 model. **Results:** CBX-12 combined with anti-PD-1 or anti-CTLA4 results in delayed tumor growth and complete response, with cured animals displaying long-term antitumor immunity. CBX-12 stimulates expression of MHC 1 and PD-L1 and is an inducer of immunogenic cell death, producing long-term immune recognition of tumor cells and resultant antitumor immunity. **Conclusion:** The authors' data provide the rationale for exploring immunotherapy combinations with CBX-12 in clinical trials.

Plain language summary: Although combinations of chemotherapy and immunotherapy have shown great promise for cancer treatment, they have also demonstrated significant safety concerns that require dose reductions. Targeting chemotherapy to the tumor can avoid these safety issues, thereby enhancing efficacy of combination therapies. CBX-12 is a novel peptide-drug agent targeting the TOP1-inhibiting drug exatecan to tumor via pH-sensitive peptide. Unlike tumor targeting via antibody, CBX-12 universally targets all solid tumors. CBX-12 avoids the immune cell toxicity of nontumor-targeted exatecan and safely synergizes with immunotherapies. CBX-12 treatment causes tumor cells to express and secrete molecules that result in activation of immune components to recognize and eliminate tumor cells. These data support the upcoming clinical trials of CBX-12 in combination with immunotherapy.

First draft submitted: 17 May 2022; **Accepted for publication**: 1 December 2022; **Published online**: 4 January 2023.

Keywords: CBX-12 • exatecan • TOP1 inhibitor • anti-PD-1 • anti-CTLA4 • immune checkpoint blockade • immunogenic cell death • immunotherapy

Although immune checkpoint inhibitors have revolutionized cancer management in a subset of patients, there is a drive to develop doublet and triplet combinations to achieve greater

efficacy. Targeted agents and cytotoxic chemotherapy can effectively synergize with immunotherapy through mechanisms that include the induction of immunogenic cell death (ICD) via the release of tumor antigens and damage-associated molecular patterns (DAMPs) from dying cells to stimulate immune cell recruitment and systemic immune cell activation as well as through immunomodulatory effects that sensitize tumor cells within immunosuppressive microenvironments to killing by immune cells [1,2]. However, immunotherapy combinations with small-molecule therapeutics can also produce synergistic toxicity, with patients undergoing combination therapy having a significantly higher risk of experiencing grade 3 or higher treatment-related adverse events such as anemia and neutropenia versus monotherapy alone [3]. The recommended phase II dose of such combinations can be lower than expected, with failure to reach the anticipated small-molecule target dose in 63% of phase I trials in combination with anti-CTLA4 and 50% of phase I trials in combination with anti-PD-L1 [4].

To enhance the therapeutic index of potent small molecules, Cybrexa Therapeutics (CT, USA) has developed the alphalex™, a pH-sensitive peptide derived from a unique variant of a family of pH-low insertion peptides [5,6]. The alphalex takes advantage of the Warburg effect, a universal feature of all tumors, to selectively deliver active payloads directly into the tumor cell cytosol without the need for a tumor-specific antigen. In low pH conditions, the peptide undergoes a conformational change to form an alpha helix, resulting in the directional insertion of a cargo across the tumor cell membrane and directly into the cytosol, where it is released via a glutathione-cleavable, self-immolating linker (Figure 1A).

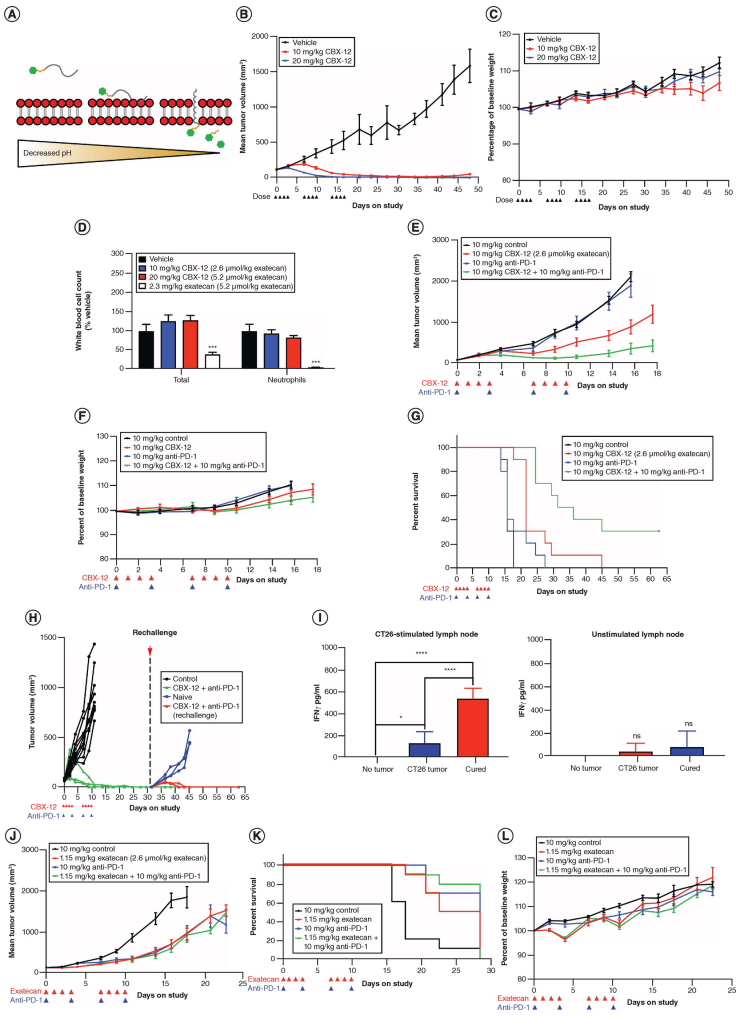

Figure 1. pH-selective tumor targeting by CBX-12 effectively synergizes with anti-PD-1 and produces long-term antitumor immunity.

(A) Schematic representation of an alphalex™ conjugate interacting with and inserting across a lipid bilayer to deliver a cargo. **(B)** Efficacy of 10 and 20 mg/kg CBX-12 dosed intraperitoneally QD×4/wk × 3 weeks in the GA2157 gastric adenocarcinoma patient-derived xenograft model. Data are expressed as mean ± standard error of the mean (SEM; n = 8 mice/arm). **(C)** Percent change in body weight of GA2157 gastric tumor-bearing animals dosed with 10 and 20 mg/kg CBX-12 QD×4/wk × 3 weeks as described in **(B).** Data are expressed as mean ± SEM. **(D)** Percent change in white blood cell counts of mice dosed QD×4 with the indicated dose of vehicle, CBX-12 or exatecan. Blood was taken 4 h after the last dose. Significance was determined with one-way analysis of variance (n = 4 mice/arm). **(E)** Efficacy of 10 mg/kg CBX-12 dosed intraperitoneally QD×4/wk × 2 weeks and 10 mg/kg anti-PD-1 dosed intraperitoneally Q4D × 4 as a single agent and in combination in the CT26 colorectal flank model. Data are expressed as mean ± SEM (n = 10 mice/arm). **(F)** Percent change in body weight of CT26 colorectal tumor-bearing animals in **(E)**. **(G)** Survival analysis of animals in the study described in **(E)** (n = 10 mice/arm). Animals were removed from the study if tumor burden was larger than 2000 mm^3 or body weight decreased more than 20%. **(H)** Spider plot of the control and three of the ten combination animals from the study described in **(E)** that demonstrated a complete response. On day 32 of the study, the three animals with a complete response were rechallenged with CT26 cells on the opposite flank. Naive animals were also injected with CT26 cells on day 32 as a control for the rechallenge. **(I)** IFN-γ secretion of single-cell suspension derived from tumor draining lymph nodes of animals from the rechallenge study described in **(H).** Lymph nodes were isolated on day 64 of the study and cocultured ± mitomycin C-inactivated CT26 cells *in vitro*. IFN-γ levels were assessed after 5 days of coculture. Lymph nodes from nontumor-bearing mice were used as an additional negative control. Data are expressed as mean ± standard deviation (n = 6). Significance was determined with one-way analysis of variance. **(J)** Efficacy of 1.15 mg/kg exatecan (equimolar to 10 mg/kg CBX-12 described in the study in **(E)**) dosed intraperitoneally QD×2/wk × 2 weeks and 10 mg/kg anti-PD-1 dosed Q4D × 4 as a single agent and in combination in the CT26 colorectal flank model. Data are expressed as mean ± SEM (n = 10 mice/group). **(K)** Survival analysis of animals in the study described in **(J).** Animals were removed from the study if tumor burden was larger than 2000 mm^3 or body weight decreased more than 20%. **(L)** Percent change in body weight of CT26 colorectal tumor-bearing animals as described in **(J).**
QD: Once daily; QDx4/wk: Once daily for 4 days each week; Q4D: Every 4 days.
*p < 0.05; ***p = 0.0001–0.001; ****p < 0.0001.

The authors have previously published the characterization of CBX-12, the alphalex conjugated to the potent TOP1 inhibitor exatecan [7]. Exatecan is a camptothecin analog that was tested in multiple clinical trials with promising initial efficacy signals; however, dose-limiting toxicities such as myelosuppression prevented its further development as a monotherapy [8–10]. CBX-12 has been shown to enhance the therapeutic index of exatecan by selectively delivering it to tumor, demonstrating efficacy and safety across multiple tumor models without the myelosuppression and gastrointestinal toxicity observed with equimolar doses of unconjugated exatecan. CBX-12 is currently in a phase I clinical trial for the treatment of advanced solid tumors (NCT04902872).

Here the authors characterize the ability of CBX-12 to effectively synergize with both anti-PD-1 and anti-CTLA4 immunotherapies in an antigen-independent manner. The authors investigate the general mechanism of action behind the observed synergy and show that CBX-12 induces immunomodulatory effects in tumor cells as well as long-term antitumor immunological memory through the induction of ICD. These findings provide the preclinical rationale for combining CBX-12 with immunotherapy in combination trials in solid tumors in the near future.

Materials & methods

Cell lines

Authenticated CT26 cells (CRL-2638; American Type Culture Collection, VA, USA) and HCT116 cells (HD-PAR-073; Horizon Discovery Ltd, Waterbeach, UK) were maintained in Dulbecco's modified Eagle medium (DMEM) supplemented with 10% fetal bovine serum (FBS), 50 IU/ml penicillin, 50 µg/ml streptomycin and 2 mM GlutaMAX (Thermo Fisher Scientific, MA, USA) at 37°C in a humidified atmosphere with 5% CO_2. Cells were subcultured twice weekly and

harvested during exponential growth for tumor inoculation. Cells were verified to be negative for mycoplasma prior to all experiments.

Xenograft experiments

All animal studies were approved by the institutional animal care and use committee. All mice were euthanized by cervical dislocation under anesthesia according to regulations in the National Research Council Guide for the Care and Use of Laboratory Animals. Mice were dosed as described in Tables 1–4 for each specific model.

Table 1. Information on each group of animals for GA2157 patient-derived xenograft experiments. (Table view)

Group	Treatment	Dose, mg/kg	Dosing schedule	Administration
1	Vehicle (5% mannitol in citrate buffer)	NA	QD×4/wk × 3	ip.
2	CBX-12	10	QD×4/wk × 3	ip.
3	CBX-12	20	QD×4/wk × 3	ip.

ip.: Intraperitoneal; NA: Not applicable. QDx4/wk: Once daily for 4 days a week.

Table 2. Information on each group of animals for CBX-12/anti-PD-1 experiments. (Table view)

Group	Treatment	Dose, mg/kg	Dosing schedule	Administration
1	Control (5% mannitol in citrate buffer and isotype control)	NA	QD×4/wk × 2 Q4D × 4	ip. ip.
2	CBX-12	10	QD×4/wk × 2	ip.
3	Anti-PD-1	10	Q4D × 4	ip.
4	CBX-12 Anti-PD-1	10 10	Q4D × 4 Q4D × 4	ip. ip.

ip.: Intraperitoneal; NA: Not applicable; QDx4/wk: Once daily for 4 days a week; Q4D: Every 4 days.

Table 3. Information on each group of animals for exatecan/anti-PD-1 experiments. (Table view)

Group	Treatment	Dose, mg/kg	Dosing schedule	Administration
1	Control (5% mannitol in citrate buffer and isotype control)	NA	QD×4/wk × 2 Q4D × 4	ip. ip.
2	Exatecan	1.15	QD×4/wk × 2	ip.
3	Anti-PD-1	10	Q4D × 4	ip.
4	Exatecan Anti-PD-1	1.15 10	Q4D × 4 Q4D × 4	ip. ip.

ip.: Intraperitoneal; NA: Not applicable; QDx4/wk: Once daily for 4 days a week; Q4D: Every 4 days.

Table 4. Information on each group of animals for CBX-12/anti-CTLA4 experiments. (Table view)

Group	Treatment	Dose, mg/kg	Dosing schedule	Administration
1	Control (5% mannitol in citrate buffer and isotype control)	NA	QD×4/wk × 2 Q4D × 4	ip. ip.

Group	Treatment	Dose, mg/kg	Dosing schedule	Administration
2	CBX-12	1.15	QD×4/wk × 2	ip.
3	Anti-CTLA4	0.5	Q4D × 4	ip.
4	CBX-12 Anti-CTLA4	1.15 0.5	Q4D × 4 Q4D × 4	ip. ip.

ip.: Intraperitoneal; NA: Not applicable; QDx4/wk: Once daily for 4 days a week; Q4D: Every 4 days.

Compound administration

Intraperitoneal doses of 10 or 20 mg/kg CBX-12 (2.6 and 5.2 µmol/kg, respectively) or 1.15 or 2.3 mg/kg exatecan (2.6 and 5.2 µmol/kg, respectively) were prepared by diluting 0.1 mg/µl dimethyl sulfoxide stocks in 5% mannitol in citrate buffer. The compound was administered each day of dosing at a volume of 12 ml/kg (300 µl per 25-g mouse). Intraperitoneal doses of 10 mg/kg RMP1-14 anti-PD-1 antibody (BE0146; Bio X Cell, NH, USA), 0.5 mg/kg 9D9 anti-CTLA4 antibody (BP0164; Bio X Cell) or anti-PD-1 or anti-CTLA4 isotype control (BE0089 and BP0086, respectively; Bio X Cell) were prepared in the appropriate antibody dilution buffers and administered at a volume of 12 ml/kg (300 µl per 25-g mouse).

Xenograft tumor growth measurements

Xenograft tumors were measured by calipers, and volume was calculated using the equation for ellipsoid volume: volume = $\pi/6 \times (\text{length}) \times (\text{width})^2$.

GA2157 gastric carcinoma patient-derived xenograft

Tumor fragments from stock mice were harvested and used for inoculation into 6- to 8-week-old female BALB/c nude mice. Each mouse was inoculated subcutaneously in the right flank with a 2- to 3-mm diameter GA2157 tumor fragment (Crown Bioscience, CA, USA) for tumor development. Tumors were then grown to a mean size of approximately 100–200 mm^3, and mice were then split into groups and treated as detailed in Table 1.

CT26 cell line-derived xenograft

6- to 7-week-old female BALB/cAnNTac mice were obtained from Taconic Biosciences, Inc. (NY, USA). Each mouse was inoculated subcutaneously with 5×10^6 CT26 tumor cells (CRL-2638; American Type Culture Collection) in 0.1 ml of phosphate-buffered saline (PBS; Thermo Fisher Scientific) with Matrigel (Corning, NY, USA) at a 1:1 ratio. Tumors were then grown to a mean size of approximately 100–200 mm^3, and mice were then split into groups and treated as detailed in Tables 2–4.

CT26 rechallenge experiment in mice cured by CBX-12/anti-PD-1 combo

Female BALB/c mice with CT26 flank syngeneic tumors were administered 10 mg/kg CBX-12 in combination with 10 mg/kg of an anti-PD-1 monoclonal antibody. CBX-12 was administered by intraperitoneal injection once daily × 4 days/week for two cycles. The anti-PD-1 antibody was administered by intraperitoneal injection on days 0, 3, 7 and 10. On day 32 of this experiment, mice that had experienced complete tumor regression (n = 3) were rechallenged by subcutaneously implanting a second inoculation of murine CT26 cancer cells in the opposite flank. Caliper measurements of potential new tumor growth were obtained on both flanks over a 32-day period until experiment termination at day 64. Naive, untreated control mice injected with murine CT26 cancer cells served as controls for the rechallenge.

CT26 vaccination & rechallenge experiment

Whole-cell vaccine preparation (CBX-12-treated CT26 cells)

Murine CT26 cells in T-150 culture flasks were treated with 30 µM CBX-12 for 3 days. To harvest the cells, tissue culture supernatants were removed, monolayers were rinsed with PBS and cells were detached with 7 ml of warm TrypLE (Thermo Fisher Scientific). Detached cells were washed with cold tissue culture medium and pelleted by centrifugation at 1200 rpm for 5 min at 4°C. Cells were washed once with 50 ml of cold calcium and magnesium-free PBS and resuspended in 3.38 ml of cold PBS for a final concentration of 30×10^6 cells/ml. Cells were kept on ice and administered to the left flank of BALB/c mice by intramuscular injection at a concentration of 0.1 ml per mouse (3×10^6 cells/mouse).

Whole-cell vaccine preparation (frozen–thawed CT26 cells)

Murine CT26 cancer cells cultured in T-150 culture flasks were rinsed with 50 ml of PBS and harvested by adding 7 ml of warm TrypLE for 2–3 min at 37°C. Detached cells were washed with cold tissue culture medium and pelleted by centrifugation at 1200 rpm for 5 min at 4°C. Cells were resuspended in PBS at a final concentration of 30×10^6 cells/ml. Cells were subjected to three freeze–thaw cycles in an ice bucket containing liquid nitrogen + methanol.

Frozen–thawed CT26 cell vaccinations were kept on ice and administered to the left flank of BALB/c mice by intramuscular injection at a concentration of 0.1 ml per mouse (3×10^6 cells/mouse). Booster vaccinations were administered 2 weeks after the initial vaccination using fresh vaccine prepared as described earlier for CBX-12-treated and frozen–thawed cells. For the rechallenge, live CT26 cells were prepared as described earlier and injected into the opposite flank 7 days after the booster vaccination.

Ex vivo assays

White blood cell quantification in mice

Female nude mice bearing HCT116 xenografts measuring approximately 300 mm^3 in size were administered intraperitoneal doses of vehicle, 10 or 20 mg/kg CBX-12 (2.5 and 5.1 µmol/kg, respectively) or 2.3 mg/kg exatecan (5.1 µmol/kg) once daily for 4 days (n = 4 mice/group). At 4 h after the final dose on day 4, mice were anesthetized via continuous inhalation of isoflurane administered in 2% oxygen. Approximately 500 µl of whole blood was collected from the heart via cardiac puncture into ethylenediaminetetraacetic acid-treated microtainers (BD Biosciences, CA, USA) on ice. Total cell count and differential were determined in whole blood using an Element HT5 Hematology Analyzer (Heska Corporation, CO, USA) as per the manufacturer's instructions.

Ex vivo lymph node & splenocyte stimulation & cytokine measurement

Axillary and inguinal tumor draining lymph nodes (DLNs) and spleens were harvested and transferred into individual Petri dish wells containing 5 ml of cold PBS for processing. Single-cell suspensions of DLNs and spleens were prepared by pressing each between frosted glass slides and passing the homogenate through a 40-µm cell strainer (CELLTREAT Scientific Products, MA, USA) into a 50-ml conical tube. The volume was adjusted to 15 ml with cold sterile PBS, and cells were pelleted by centrifugation at 1200 rpm for 5 min at 4°C. The supernatant was removed and cells were resuspended in cold Roswell Park Memorial Institute (RPMI) 1640 (Cytiva, UT, USA) supplemented with 10% heat-inactivated FBS, 10 U/ml penicillin, 10 µg/ml streptomycin, 1× GlutaMAX, 10 mM HEPES (Thermo Fisher Scientific) and

50 µM β-mercaptoethanol (Thermo Fisher Scientific). Cell suspensions were adjusted to 1×10^6 cells/ml in RPMI 1640.

DLN cells and splenocyte preparations (effector cells) were plated into Falcon 96-well flat-bottom tissue culture plates (3653025; Corning) at a volume of 100 µl/well (1×10^5 cells). CT26 cells (stimulator cells) were pretreated with 30 µM mitomycin C for 2½ h, extensively washed and then added at an effector-to-stimulator ratio of 5:1. Tissue culture supernatants were harvested at various time points to determine murine IL-2 and IFN-γ production by ELISA (R&D Systems, MN, USA).

Intratumoral tumor-infiltrating lymphocyte FACS analysis

Syngeneic CT26 tumors were removed from the flank and placed in Petri dishes on ice. The solid tumors were immediately minced with scissors followed by the addition of 3 ml tumor dissociation enzyme mix (Miltenyi Biotec, CA, USA). The suspension was incubated for 40 min at 37°C on a shaker. An equal volume of cold DMEM complete medium was added to each sample, which was passed through a 40-µm mesh cell strainer and subsequently passed through a 70-µm cell strainer. The single-cell suspensions were pelleted and resuspended to a concentration of 3×10^6 cells/ml in cold flow wash buffer (FWB), and 100 µl of each sample was added to the wells of a round-bottom polypropylene plate for cell staining.

CT26 tumor cell suspensions were pelleted and washed once with cold FWB at 200 µl/well. The cell pellets were stained in 100 µl of cold FWB containing either anti-mouse CD45–allophycocyanin or isotype control antibody–allophycocyanin (BD Biosciences, CA, USA) and incubated for 30 min in the dark at 4°C. The antibody-labeled cells were washed and then resuspended in a 200-µl volume of FWB and read on a BD Accuri C6 Sampler Flow Cytometer (BD Biosciences).

Derivation & stimulation of bone marrow-derived dendritic cells

Bone marrow-derived dendritic cells (DCs) were differentiated from the bone marrow obtained from the femurs of female BALB/c mice (The Jackson Laboratory, ME, USA). The ends of the bones were snipped, and bone marrow was extruded by flushing with a 23-gauge needle containing cold PBS. The bone marrow preparations were dispersed by gentle pipetting up and down, and cell aggregates were removed by passing through 70-µm cell strainers. The cell preparations were washed once with cold PBS; resuspended in RPMI 1640 supplemented with 10% FBS containing 100 U/ml penicillin, 100 µg/ml streptomycin and 10 mM HEPES; and counted using trypan blue exclusion. Viable cells were readjusted to 2.0×10^6/ml in complete medium supplemented with 40 ng/ml murine GM-CSF (R&D Systems). The cells were then transferred to a T-150 flask and cultured for 11 days in a humidified chamber at 37°C and 5% CO_2. On days 4, 6 and 8, half of the medium was removed and replaced with fresh complete medium supplemented with 40 ng/ml GM-CSF.

After 11 days of culture, nonadherent cells were harvested, washed and resuspended in complete medium containing 40 ng/ml murine GM-CSF at 2.0×10^6/ml. Next, 1 ml of DCs was added to each well of a 24-well plate followed by the addition of 1 ml of medium supplemented with 40 ng/ml murine GM-CSF containing 2.0×10^6/ml CBX-12-treated CT26 cells as previously described or complete medium alone to serve as the nonstimulated control group. Cells were incubated for 24 h in a humidified chamber at 37°C and 5% CO_2 and then harvested for FACS to determine the degree of activation. DC activation was indicated by an increase in cell surface CD86 expression. DCs were harvested and resuspended in cold PBS containing 2% FBS and 0.02% w/v sodium azide (FWB). Immunofluorescence staining of DCs

was conducted in 96-well round-bottom plates containing 100 µl of antibody. CD86 expression was assessed with a CD86-specific antibody (clone GL1) and clone R35-95 isotype control antibody (BD Biosciences). After 30 min of incubation on ice, cells were washed with FWB and analyzed using a BD Accuri C6 Plus Flow Cytometer (BD Biosciences). A total of 10,000 events were collected and analyzed using forward scatter versus side scatter and FL4 fluorescence, and data were analyzed using BD CSampler Plus software (BD Biosciences).

In vitro assays

Assessment of cell surface PD-L1 or MHC I by FACS

Murine CT26 cells were harvested with TrypLE, washed and resuspended in DMEM complete medium. Subsequently, 1.5×10^6 cells in 20 ml medium were transferred to a T-75 flask and cultured for 2 h in a humidified chamber at 37°C and 5% CO_2 to allow for cell adherence. The compound was added at various concentrations, and cultures were incubated for 24 h for exatecan and 72 h for CBX-12. Monolayers were harvested with TrypLE, washed and resuspended to a concentration of 3.0×10^6/ml in Ca/Mg-free PBS. Cells were plated to a total volume of 100 µl and incubated with a 1:1000 dilution of LIVE/DEAD Green cell stain (Thermo Fisher Scientific) in Ca/Mg-free PBS buffer for 30 min at room temperature in 96-well round-bottom polypropylene plates. Cells were washed with cold PBS; resuspended in 100 µl FWB consisting of PBS, 2% FBS and 0.02% sodium azide (VWR International, LLC, PA, USA); and blocked with Fc block (BD Biosciences) at 200 µg/ml for 5 min at 4°C. CT26 cells were stained with either rat anti-mouse PD-L1 (BD Biosciences) or rat anti-mouse MHC class I (BioLegend, CA, USA) in cold FWB for 30 min at 4°C. After incubation, the cells were washed and resuspended in 200 µl of cold FWB. Gating strategy was set on the live cells identified using LIVE/DEAD staining, and PD-L1 and MHC I staining was recorded for each sample using the BD Accuri C6 Sampler Flow Cytometer.

Detection of extracellular ATP

Extracellular release of ATP was detected in tissue culture supernatants using a RealTime-Glo Extracellular ATP luminescence kit (Promega Corporation, WI, USA) according to the manufacturer's instructions. Briefly, 200 µl of tumor cell lines was seeded (1563 cells/well) into 96-well flat-bottom solid white tissue culture plates and incubated overnight in a humidified chamber at 37°C and 5% CO_2. Tissue culture supernatant (50 µl) was removed, and 50 µl of compound was added to each well to produce the indicated final concentration. Cells were then incubated for an additional 24 h. Next, 10 µl of a 20× concentration of RealTime Glo luminescent reagent reconstituted in DMEM complete medium was added to each well, and the cultures were monitored for extracellular ATP release over the next 24 h in a humidified chamber at 37°C and 5% CO_2 using a Cytation 3 luminescence reader (BioTek Instruments, VT, USA) for kinetic analysis.

Detection of secreted HMGB1

Tumor cells were harvested as described earlier and resuspended at 1×10^5/ml in DMEM complete medium. Resuspended cells (2 ml/well) were added to a 24-well plate, and compound diluted in dimethyl sulfoxide was added to the wells at the indicated final concentrations. Cells were cultured in a humidified chamber at 37°C and 5% CO_2 for 72 h. Tissue culture supernatants were harvested at 24, 48 and 72 h; stored at 80°C; and thawed immediately prior to analysis. Tissue culture supernatants were monitored for human and

murine HMGB1 release by a single cross-reactive commercial ELISA kit (Tecan, Männedorf, Switzerland) according to the manufacturer's instructions.

Statistical analysis

Analysis of variance was used to test for significant differences between groups. *Post hoc* Bonferroni multiple comparison test analysis was used to determine significant differences among means. All statistical analyses were accomplished using Prism 8.2.0 software (GraphPad Software, Inc., CA, USA).

Results

Antigen-independent tumor targeting by the alphalex™–exatecan conjugate CBX-12 induces synergy with anti-PD-1

CBX-12 is a peptide-drug conjugate designed to enhance the therapeutic window of the potent TOP1 inhibitor exatecan by selectively delivering this warhead to the tumor over healthy tissues [7]. Efficacious doses of CBX-12, which produce complete regression in a gastric tumor patient-derived xenograft model, do not display the severe neutropenia produced by equimolar doses of unconjugated exatecan (Figure 1B & D). Concordantly, no signs of body weight loss are observed with CBX-12 treatment (Figure 1C).

Given the efficacy of CBX-12 in multiple models both as a single agent and in combination [7], the authors first tested the ability of CBX-12 to safely and effectively synergize with anti-PD-1 immunotherapy in BALB/c mice bearing syngeneic HER2-negative CT26 colorectal flank tumors. Mice were dosed intraperitoneally with two 4-day cycles of CBX-12 at 10 mg/kg and one dose of anti-PD-1 at 10 mg/kg every 4 days for four total doses as a single agent or in combination (Figure 1E & F). The authors found that although the anti-PD-1 antibody alone had minimal antitumor activity in this experiment, the combination of CBX-12 and anti-PD-1 had a synergistic effect, significantly delaying tumor growth and increasing survival, with three of ten animals in the combination group having a prolonged complete response that lasted until study completion on day 64 (Figure 1G & H).

To determine whether combination treatment results in the formation of immunological memory against CT26 tumor cells, on day 32 of this combination study, the three animals in complete response were rechallenged with CT26 cells on the opposite flank without any subsequent drug treatment. Although CT26 cells injected into control naive mice rapidly formed progressive tumors, rechallenged mice developed small tumors that rapidly and completely regressed up to study completion on day 64 (Figure 1H).

To further confirm antitumor immunological memory against CT26 cells *ex vivo*, tumor DLNs of rechallenged and control mice were isolated on day 64, and lymph node cells were stimulated with and without nonproliferating mitomycin C-treated CT26 cells. Mitomycin C pretreatment is required to avoid continued replication of CT26 cells *in vitro*. Because of their rapid growth, CT26 cells would otherwise rapidly overtake lymph node-derived cells. After 5 days of coculture, IFN-γ in the supernatant was measured by ELISA (Figure 1I). Suspensions from lymph nodes derived from all tumor-bearing animals displayed slight nonsignificant secretion of IFN-γ even without *ex vivo* stimulation by CT26 cells, concordant with the slightly immunogenic nature of the tumors *in vivo*. Importantly, secretion of IFN-γ increased with *ex vivo* stimulation, with lymph nodes from cured rechallenged mice having nearly fourfold induction of IFN-γ relative to naive CT26 tumor-bearing controls.

Given the systemic and indiscriminate impact of unconjugated exatecan on healthy cells, including circulating and tumor-infiltrating immune cells, the authors hypothesized that a

combination of unconjugated exatecan and anti-PD-1 would not display the same degree of synergistic antitumor activity relative to CBX-12 treatment. In fact, an equimolar dose of unconjugated exatecan relative to CBX-12 failed to show either synergistic or additive activity in combination with anti-PD-1 (Figure 1J & K). As expected, exatecan treatment was accompanied by increased toxicity, as evidenced by decreases in body weight that resolved after the dosing period (Figure 1L). Conversely, weight loss was not observed with the equimolar CBX-12 dose (Figure 1F). Together, these data show that anti-PD-1 combined with CBX-12, but not with unconjugated exatecan, demonstrates synergistic activity, producing specific and long-term antitumor immunological memory that results in a complete response.

CBX-12 induces cancer cell surface expression of PD-L1 & MHC I & enhances intratumoral leukocyte infiltration

The authors next interrogated the mechanism of synergy between CBX-12 and anti-PD-1 immunotherapy in CT26 cells. TOP1 inhibitors and other DNA damage-inducing agents have been reported to induce cancer cell surface expression of immunomodulatory molecules such as PD-L1 and increase expression of MHC I antigen presentation in a dose-dependent manner, providing the rationale for their combination with immunotherapy in the clinic [11,12]. Response to immune checkpoint blockade is mediated in large part by effector T cells, which are activated upon recognition of the cognate antigen presented on MHC 1 molecules on the surface of cancer cells along with binding of costimulatory signals [13]. Consequently, loss of MHC I expression has been correlated with resistance to immune checkpoint blockade [14,15]. MHC I induction may therefore serve to enhance T-cell activation and recognition of tumor cells, making them more susceptible to cytotoxic T-cell killing [16,17]. Conversely, compensatory upregulation of the inhibitory checkpoint ligand PD-L1 may require counteraction by anti-PD-1 antibodies to reinvigorate exhausted T cells and promote maximal antitumor immunity. The authors confirmed *in vitro* that CBX-12 was able to induce cancer cell surface expression of both PD-L1 and MHC I in a dose-dependent manner in murine CT26 cells (Figure 2A & B). This upregulation of PD-L1 and MHC I expression was also seen with unconjugated exatecan (Figure 2C & D).

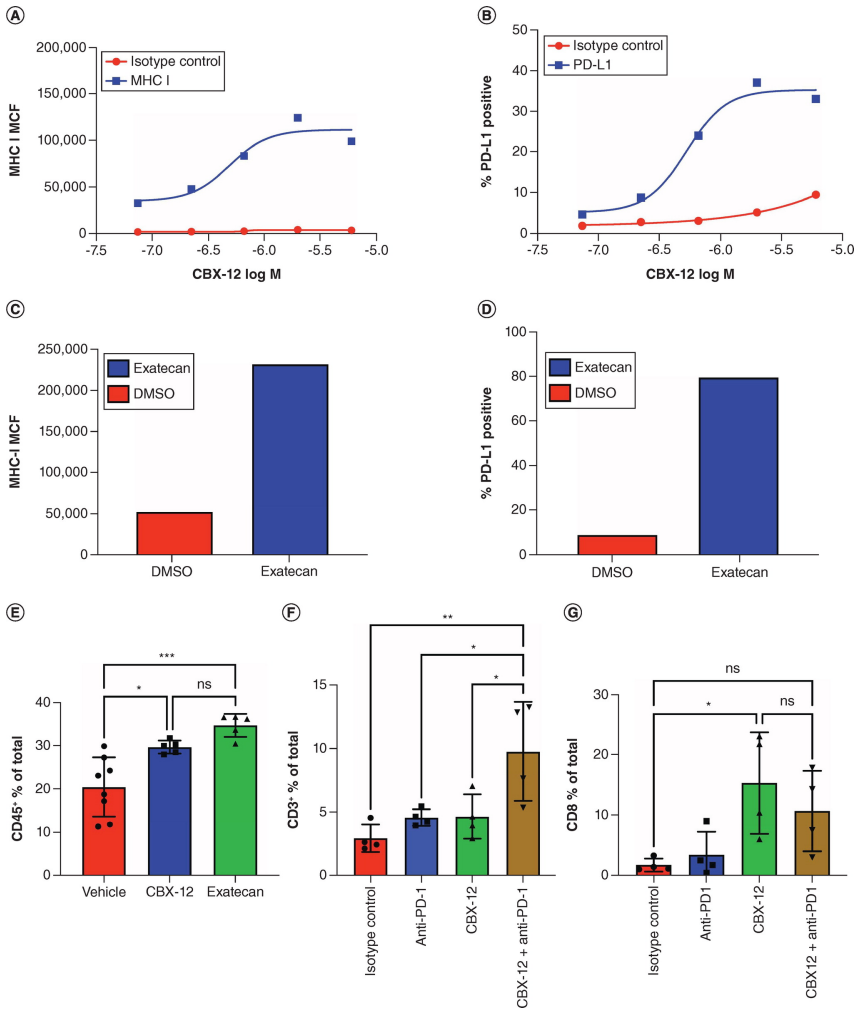

Figure 2. Induction of cell surface PD-L1 and MHC I and intratumoral lymphocyte infiltration.
(A) Induction of cell surface MHC I in CT26 cells treated for 72 h with CBX-12 and assessed by FACS. Depicted are the median channel fluorescence values after staining with either an anti-MHC I antibody or isotype control (n = 1). **(B)** Induction of cell surface PD-L1 in CT26 cells treated for 72 h with CBX-12 and assessed by FACS. Depicted is the percentage of positive cells relative to the total population after staining with either an anti-PD-L1 antibody or isotype control (n = 1). **(C)** Induction of cell surface MHC I in CT26 cells treated for 24 h with dimethyl sulfoxide or 40 nM exatecan and assessed by FACS (n = 1). **(D)** Induction of cell surface PD-L1 in CT26 cells treated for 24 h with dimethyl sulfoxide or 40 nM exatecan and assessed by FACS (n = 1). **(E)** FACS analysis of percent $CD45^+$ expression relative to the total population in single-cell suspensions derived from CT26 tumors of animals dosed intraperitoneally for four days with vehicle, 10 mg/kg CBX-12 or 1.15 mg/kg exatecan (equimolar to 10 mg/kg CBX-12). Tumors were taken for analysis 4 days after the last dose. Data are expressed as mean ± standard deviation (n = 5–8). Significance was determined with one-way analysis of variance. **(F)** FACS analysis of percent $CD3^+$ cells relative to the total population in single-cell suspensions derived from CT26 tumors of animals dosed intraperitoneally QD × 4 with isotype control, 10 mg/kg anti-PD-1, 10 mg/kg CBX-12 or a combination of anti-PD-1 and CBX-12. Significance was determined with one-way analysis of variance. Data are expressed as mean ± standard deviation (n = 4). **(G)** FACS analysis of percent $CD45^+$ $CD8^+$ cells relative to the total population in single-cell suspensions derived from CT26 tumors of animals dosed intraperitoneally QD × 4 with isotype control, 10 mg/kg anti-PD-1, 10 mg/kg CBX-12 or a combination of anti-PD-1 and CBX-12 in an independent experiment from **(F)**. Significance was determined with one-way analysis of variance. Data are expressed as mean ± standard deviation (n = 4).
*p < 0.05; **p < 0.01; ***p = 0.0001–0.001.

The authors then studied tumor-infiltrating lymphocytes (TILs) after dosing CT26 tumor-bearing mice with one 4-day cycle of either 10 mg/kg of CBX-12 or the equimolar 1.15-mg/kg dose of unconjugated exatecan. Both CBX-12 and exatecan induced significant infiltration of $CD45^+$ leukocytes into the tumor microenvironment (Figure 2E). In a separate experiment profiling TILs after one 4-day cycle of the anti-PD-1 and CBX-12 combination, the authors found that although tumors from the anti-PD-1 and CBX-12 monotherapy arms trended toward a higher number of $CD3^+$ TILs, the combination of anti-PD-1 and CBX-12 induced a

significant increase in $CD3^+$ TILs relative to all other groups (Figure 2F). Further analysis of TIL subsets in an independent experiment showed that the combination of CBX-12 and anti-PD-1 resulted in a trend toward increased $CD45^+CD8^+$ T cells in line with the overall increase in $CD3^+$ T cells, whereas CBX-12 monotherapy induced a more specific $CD8^+$ cytotoxic T-cell recruitment (Figure 2G).

CBX-12 induces synergy with anti-CTLA4

Given the induction of MHC 1 and increased TILs prompted by CBX-12, the authors next examined whether CBX-12 could demonstrate synergy outside of the PD-L1 axis by testing for efficacy with combined anti-CTLA4 immunotherapy in the CT26 flank model. The authors found that the combination of CBX-12 and anti-CTLA4 enhanced antitumor activity relative to either monotherapy alone (Figure 3A & B). Of note, the combination group displayed a dichotomous response, with four of ten animals exhibiting clear synergistic activity and complete tumor regression lasting for nearly 2 weeks (synergistic responders), translating into increased survival (Figure 3C & D). In the synergistic responder group, the time to quadruple the initial starting tumor volume was ten times longer than that observed in the control group, demonstrating that CBX-12 synergizes with anti-CTLA4 in addition to anti-PD-1 (Figure 3E).

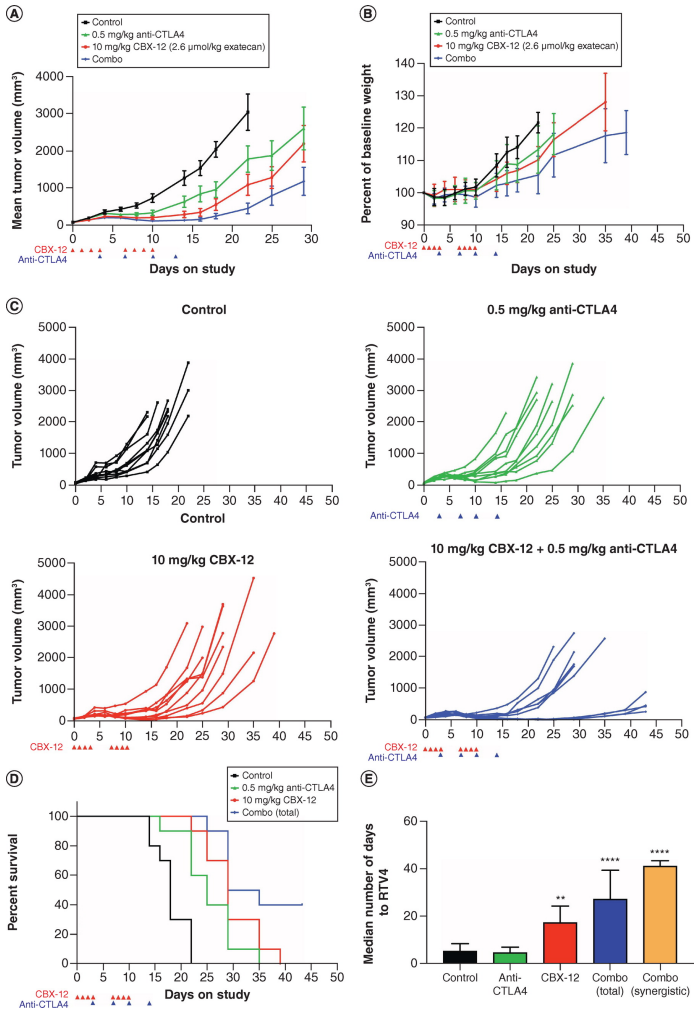

Figure 3. Synergy of CBX-12 combined with anti-CTLA4.
(A) Efficacy of 10 mg/kg CBX-12 dosed intraperitoneally QD × 4/wk × 2 weeks and 0.5 mg/kg anti-CTLA4 dosed intraperitoneally Q4D × 4 as a single agent and in combination in the CT26 colorectal flank model. Data are expressed as mean ± standard error of the mean (n = 10 mice/arm). **(B)** Percent change in body weight of CT26 colorectal tumor-bearing animals dosed with 10 mg/kg CBX-12 QD × 4/wk × 2 weeks and 0.5 mg/kg anti-CTLA4 Q4D × 4 as a single agent and in combination as described in **(A)**. **(C)** Spider plots of the efficacy experiment described in **(A)**. **(D)** Survival analysis of animals in the study described in **(A)**. Animals were

removed from the study if tumor burden was larger than 2000 mm ^{3} or body weight decreased more than 20%. **(E)** Effect of CBX-12 and anti-CTLA4 on median number of days to reach four times initial starting tumor volume (RTV4) in the efficacy study described in **(A)**. A subset of animals comprising the synergistic response group was pulled from the total combination group and analyzed separately. Data are expressed as mean ± standard deviation. Significance was determined with one-way analysis of variance.
**p < 0.01; ****p < 0.0001.
QDx4/wk: Once daily for 4 days a week; Q4D: Every 4 days; RTV4: Four times the initial tumor volume.

CBX-12 induces long-term antitumor immunological memory through the induction of ICD

Although some TOP1 inhibitors are reported to induce ICD [18], to date, the specific activity of exatecan as an ICD inducer has not been reported. The authors measured levels of ATP and HMGB1, which are the most consistently upregulated DAMPs in a broad range of experiments and cell lines in response to both chemical- and physical stress-induced ICD [19,20]. Unconjugated exatecan induced human HCT116 colorectal cell secretion of both HMGB1 and ATP into the culture medium (Figure 4A & B). Similar results were also seen with CBX-12, which displayed dose-dependent secretion of ATP and HMGB1 that was right-shifted (as expected) in neutral buffered cell culture medium relative to the response observed with exatecan (Figure 4C & D).

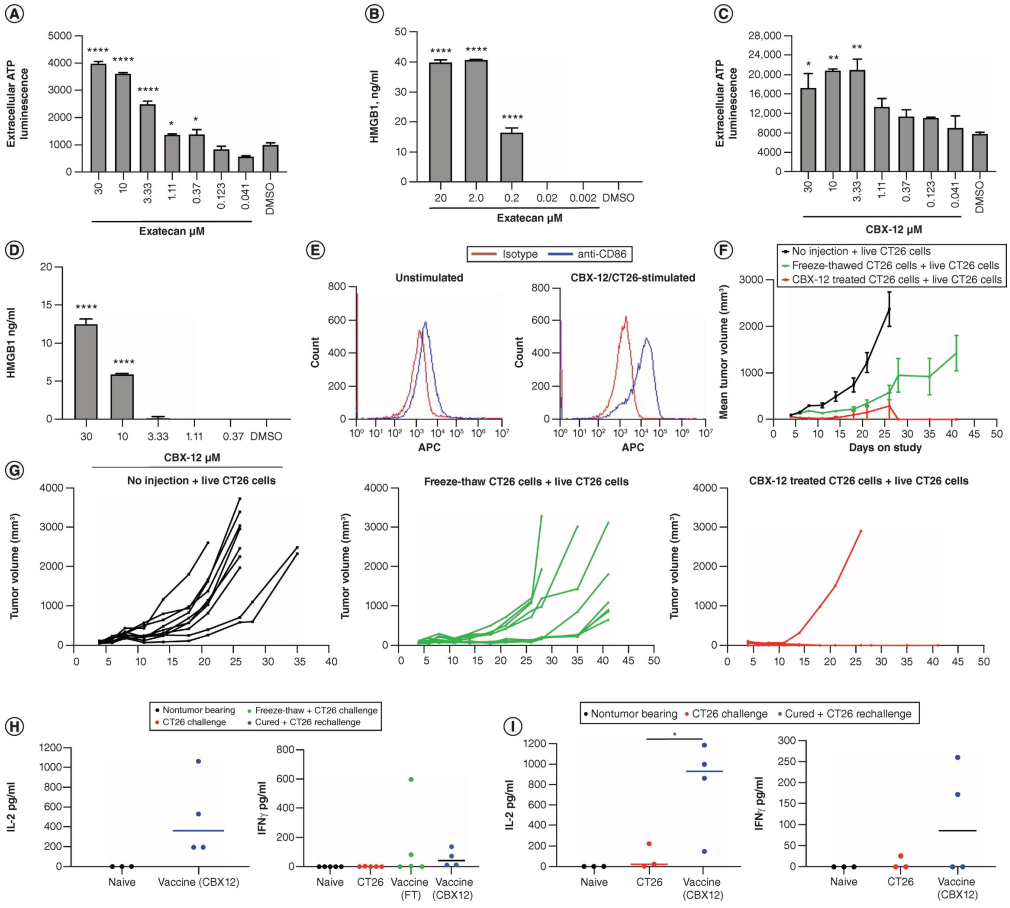

Figure 4. Induction of immunogenic cell death by CBX-12.
(A) Induction of extracellular ATP *in vitro* after exposure of HCT116 cells to exatecan for 19 h (n = 2). **(B)** Secretion of HMGB1 into culture medium as assessed by ELISA after exposure of HCT116 cells to exatecan for 48 h (n = 2). **(C)** *In vitro* induction of extracellular ATP after exposure of CT26 cells to CBX-12 for 45 h (n = 2). **(D)** *In vitro* secretion of HMGB1 into culture medium as assessed by ELISA after exposure of CT26 cells to CBX-12 for 72 h (n = 2). **(A–D)** Data are expressed as mean ± standard deviation (n = 2). Significance was determined with one-way analysis of variance. **(E)** Expression of CD86 on bone marrow-derived dendritic cells stimulated with and without CBX-12-treated CT26 cells for 24 h. Inset displays median channel fluorescence and percentage of positively stained cells. **(F)** Growth of CT26 tumors in BALB/c mice vaccinated with cells killed *in vitro* by either freeze–thaw or exposure to CBX-12. Animals were reinjected with live CT26 cells on the opposite flank 7 days post-vaccination. Naive unvaccinated animals injected with live CT26 cells were used as

a control. Data are expressed as mean ± standard error of the mean (n = 10). **(G)** Spider plots of the vaccination experiment described in **(F).** Nine of ten animals vaccinated by CBX-12-killed cells did not develop tumors, whereas all animals in other groups developed tumors. **(H)** Levels of IL-2 and IFN-γ secreted into culture medium after coincubation of mitomycin C-inactivated CT26 cells with single-cell suspension derived from tumor draining lymph nodes of animals from the experiment described in **(F)** . Lymph nodes were isolated from animals 22 days post-vaccination. Lymph nodes from naive nontumor-bearing animals were used as a negative control. **(I)** Levels of IL-2 and IFN-γ secreted into culture medium after coincubation of mitomycin C-inactivated CT26 cells with single-c ell suspension derived from splenocytes of animals from the experiment described in **(F)** . Splenocytes were isolated from animals 22 days post-vaccination. Splenocytes from naive nontumor-bearing animals were used as a negative control. Significance was determined with one-way analysis of variance.
*p < 0.05; **p < 0.01; ****p < 0.0001.

To further demonstrate that the release of DAMPs by CBX-12-treated CT26 cells correlated with functional activity, the authors next tested whether bone marrow-derived immature DCs transitioned to become mature, activated cells after stimulation with CT26 cells killed *in vitro* by exposure to CBX-12. After 24 h of coincubation, a significant increase in CD86 expression was observed in DCs stimulated with CBX-12-killed CT26 cells, as assessed by a 61% increase in the number of cells expressing the activation marker and a fivefold increase in CD86 median channel fluorescence (Figure 4E).

To conclusively demonstrate whether CBX-12 was a true ICD inducer *in vivo*, the authors performed a vaccination assay, which is the gold standard for determination of ICD [1,20]. BALB/c mice were vaccinated with CT26 cells killed *in vitro* by either freeze-thaw or exposure to CBX-12. Subsequently, mice were rechallenged with live CT26 cells on the opposing flank 7 days post-vaccination (Figure 4F). Although vaccination with frozen–thawed cells produced some delay in tumor growth relative to the unvaccinated control group, all animals in this group developed tumors. By contrast, nine of ten animals vaccinated with cells killed by CBX-12 failed to develop tumors after more than 40 days of monitoring, demonstrating that CBX-12 is indeed a true inducer of ICD (Figure 4G).

To confirm the formation of specific immunological memory against CT26 tumor cells, tumor DLNs and splenocytes were isolated from vaccinated mice at the end of the monitoring period. Single-cell suspensions generated from these tissues were cocultured with mitomycin C-treated CT26 cells and tested for secretion of immunostimulatory cytokines. DLN cells isolated from mice cured by the CBX-12-killed CT26 cell vaccination displayed a trend toward increased IL-2 and IFN-γ upon *ex vivo* exposure to inactivated CT26 cells (Figure 4H). In parallel, splenocytes from these animals showed a significant increase in IL-2 and a trend toward increased IFN-γ upon *ex vivo* exposure to CT26 cells (Figure 4I). By contrast, animals vaccinated with frozen–thawed cells produced only a slight induction in these cytokines upon CT26 re-exposure, which did not reach statistical significance, correlating with the ability of the frozen–thawed vaccination to produce only a slight delay in the tumor growth observed *in vivo* rather than the true antitumor immunity produced by the CBX-12-killed vaccination. Together, these *in vivo* and *ex vivo* data confirm that CBX-12 as a single agent can induce antitumor immunological memory through ICD.

Discussion

This study characterizes the ability of the pH-dependent alphalex–exatecan conjugate CBX-12 to synergize with anti-PD-1 and anti-CTLA4 immunotherapies. Here the authors demonstrate that CBX-12 can enhance intratumoral T-cell infiltration and induce systemic, long-term antitumor immunological activity both as a single agent and in combination with immunotherapy, resulting in resistance to tumor rechallenge as well as induction of

immunostimulatory cytokines in tissues *ex vivo*. Conversely, equimolar doses of unconjugated exatecan did not produce synergy with an anti-PD-1 antibody. Further work will explore the differences in intratumoral composition after treatment with CBX-12 or exatecan to elucidate the mechanism behind the lack of synergy with exatecan. Like other TOP1 inhibitors, unconjugated exatecan induces dose-limiting myelosuppression, which is avoided by CBX-12 at efficacious doses [7]. It is possible that the bone marrow toxicity induced by unconjugated exatecan could have a negative impact on T-cell lymphopoiesis and the development of naive T cells. It is also possible that, like other TOP1 inhibitors, unconjugated exatecan systemically induces apoptosis of activated, rapidly dividing lymphocytes [21].

CBX-12 has the novel advantage over antibody–drug conjugates of being able to deliver the potent TOP1 inhibitor exatecan selectively to the tumor in an antigen-agnostic manner. Deruxtecan, a less potent derivative of exatecan, has recently demonstrated efficacy in relapsed/refractory populations when delivered by the HER2-targeting antibody trastuzumab [22,23]. Enhertu (fam-trastuzumab deruxtecan-nxki; Daiichi Sankyo, Tokyo, Japan and AstraZeneca, Cambridge, UK) has been approved in metastatic HER2-positive breast cancer and is currently undergoing clinical trials in combination with immunotherapy in HER2-positive solid tumors. HER2-targeting drugs such as Enhertu are limited to a smaller subset of patients who express the HER2 antigen at sufficient levels for efficient targeting. Therefore, CBX-12 represents a universal opportunity to safely deliver a potent warhead with proven clinical activity to all solid tumors with a simple and scalable pH-sensitive peptide, rendering it widely amenable to combination with immunotherapy.

Conclusion

The authors demonstrate that antigen-independent targeting of the TOP1 inhibitor exatecan to the tumor with a pH-sensitive peptide (CBX-12) produces both superior safety and synergy with immunotherapy compared with unconjugated exatecan. CBX-12 was able to synergize with both anti-PD-1 and anti-CTLA4 immunotherapies, producing complete responses. Animals undergoing a complete response exhibited long-term antitumor immunological memory with tumor rechallenge *in vivo* and in *ex vivo* lymph nodes. Mechanistically, CBX-12 induced cell surface expression of MHC I and PD-L1 as well as tumor infiltration by $CD8^+$ T cells. CBX-12 also induced expression of DAMPs indicative of the induction of ICD. Concordantly, CBX-12 induction of tumor ICD induced the maturation of DCs *ex vivo* and demonstrated the ability to vaccinate animals against tumor cell growth *in vivo*. Together, these data provide the rationale for exploring immunotherapy combinations with CBX-12 in clinical trials.

Summary points

- Immunotherapy combinations with cytotoxins can be limited by synergistic toxicities produced by indiscriminate exposure of cytotoxins to healthy cells, including immune cells.
- CBX-12 is a novel peptide-drug conjugate that delivers the TOP1 inhibitor exatecan directly to tumor cells via pH-sensitive peptide, thereby avoiding toxicity to healthy cells.
- In contrast to antibody–drug conjugates, delivery of exatecan via pH-sensitive peptide allows CBX-12 to universally target all solid tumors.
- Superior synergy of CBX-12 over untargeted exatecan is demonstrated in combination with immunotherapy in the CT26 colorectal model.
- CBX-12 avoids toxicity to immune cells while enhancing intratumoral infiltration of $CD8^+$ T cells.
- CBX-12 synergizes with immunotherapies by stimulating tumor cell surface expression of MHC 1

and PD-L1.

- The mechanism behind long-term antitumor immunity and immunological memory induced by CBX-12 is immunogenic cell death.
- CBX-12 represents a universal opportunity to safely deliver a potent warhead with proven clinical activity to all solid tumors with a simple and scalable pH-sensitive peptide, rendering it widely amenable to combination with immunotherapy.

Author contributions

S Gayle, T Paradis, K Jones and VM Paralkar contributed to the design and implementation of the study. S Gayle, T Paradis, VM Paralkar and J Vasquez contributed to the data analysis and interpretation of the results and to the writing of the manuscript.

Financial & competing interests disclosure

S Gayle, T Paradis, K Jones and VM Paralkar are employees of Cybrexa Therapeutics. J Vasquez is funded in part by the Robert Wood Johnson Harold Amos Medical Faculty Development Program and the Fund to Retain Clinical Scientists at Yale and is sponsored by the Doris Duke Charitable Foundation (award no. 2015216) and Yale Center for Clinical Investigation. The authors have no other relevant affiliations or financial involvement with any organization or entity with a financial interest in or financial conflict with the subject matter or materials discussed in the manuscript apart from those disclosed.

No writing assistance was utilized in the production of this manuscript.

Ethical conduct of research

The authors state that they have obtained appropriate institutional review board approval or have followed the principles outlined in the Declaration of Helsinki for all human or animal experimental investigations. In addition, for investigations involving human subjects, informed consent has been obtained from the participants involved.

References

Papers of special note have been highlighted as: • of interest; •• of considerable interest

1. Fucikova J, Kepp O, Kasikova L et al. Detection of immunogenic cell death and its relevance for cancer therapy. *Cell Death Dis.* 11(11), 1013 (2020).
2. Kersten K, Salvagno C, de Visser KE. Exploiting the immunomodulatory properties of chemotherapeutic drugs to improve the success of cancer immunotherapy. *Front. Immunol.* 6, 516 (2015).
3. Zhou X, Yao Z, Bai H et al. Treatment-related adverse events of PD-1 and PD-L1 inhibitor-based combination therapies in clinical trials: a systematic review and meta-analysis. *Lancet Oncol.* 22(9), 1265–1274 (2021).
4. Simmet V, Eberst L, Marabelle A, Cassier PA. Immune checkpoint inhibitor-based combinations: is dose escalation mandatory for phase I trials? *Ann. Oncol.* 30(11), 1751–1759 (2019).
5. Wyatt LC, Lewis JS, Andreev OA, Reshetnyak YK, Engelman DM. Applications of pHLIP technology for cancer imaging and therapy. *Trends Biotechnol.* 35(7), 653–664 (2017).
   •• **Review of the applications of pH-low insertion peptide (pHLIP) technology.**
6. Wyatt LC, Moshnikova A, Crawford T, Engelman DM, Andreev OA, Reshetnyak YK. Peptides of pHLIP family for targeted intracellular and extracellular delivery of cargo molecules to tumors. *Proc. Natl Acad. Sci. USA* 115(12), e2811–e2818 (2018).
   •• **Biophysical characterization of pH-dependent insertion of pHLIP variants.**
7. Gayle S, Aiello R, Leelatian N et al. Tumor-selective, antigen-independent delivery of a pH sensitive peptide-topoisomerase inhibitor conjugate suppresses tumor growth without systemic toxicity. *NAR Cancer* 3(2), zcab021 (2021).
   •• **First report of tumor-selective targeting, safety and efficacy of CBX-12 in preclinical models.**

8. Thomas A, Pommier Y. Targeting topoisomerase I in the era of precision medicine. *Clin. Cancer Res.* 25(22), 6581–6589 (2019).
   •• **Comprehensive review of therapeutic modalities targeting TOP1.**
9. Ajani JA, Takimoto C, Becerra CR et al. A phase II clinical and pharmacokinetic study of intravenous exatecan mesylate (DX-8951f) in patients with untreated metastatic gastric cancer. *Invest. New Drugs* 23(5), 479–484 (2005).
10. Rowinsky EK. Preclinical and clinical development of exatecan (DX-951f). In: *Camptothecins in Cancer Therapy*. Adams VR, Burke TG (Eds). Humana Press, NJ, USA, 317–341 (2005).
    • **Complete review of the preclinical and clinical development of exatecan by Daiichi Pharmaceutical.**
11. Sato H, Niimi A, Yasuhara T et al. DNA double-strand break repair pathway regulates PD-L1 expression in cancer cells. *Nat. Commun.* 8(1), 1751 (2017).
12. Iwai T, Sugimoto M, Wakita D, Yorozu K, Kurasawa M, Yamamoto K. Topoisomerase I inhibitor, irinotecan, depletes regulatory T cells and up-regulates MHC class I and PD-L1 expression, resulting in a supra-additive antitumor effect when combined with anti-PD-L1 antibodies. *Oncotarget* 9(59), 31411–31421 (2018).
13. Ribas A, Wolchok JD. Cancer immunotherapy using checkpoint blockade. *Science* 359(6382), 1350–1355 (2018).
14. Lee JH, Shklovskaya E, Lim SY et al. Transcriptional downregulation of MHC class I and melanoma de-differentiation in resistance to PD-1 inhibition. *Nat. Commun.* 11(1), 1897 (2020).
15. Gettinger S, Choi J, Hastings K et al. Impaired HLA class I antigen processing and presentation as a mechanism of acquired resistance to immune checkpoint inhibitors in lung cancer. *Cancer Discov.* 7(12), 1420–1435 (2017).
16. Taylor BC, Balko JM. Mechanisms of MHC-I downregulation and role in immunotherapy response. *Front. Immunol.* 13, 844866 (2022).
17. Hazini A, Fisher K, Seymour L. Deregulation of HLA-I in cancer and its central importance for immunotherapy. *J. Immunother. Cancer* 9(8), e002899 (2021).
18. Bezu L, Gomes-de-Silva LC, Dewitte H et al. Combinatorial strategies for the induction of immunogenic cell death. *Front. Immunol.* 6, 187 (2015).
19. Kepp O, Senovilla L, Vitale I et al. Consensus guidelines for the detection of immunogenic cell death. *Oncoimmunology* 3(9), e955691 (2014).
20. Galluzzi L, Vitale I, Warren S et al. Consensus guidelines for the definition, detection and interpretation of immunogenic cell death. *J. Immunother. Cancer* 8(1), e000337 (2020).
21. Ferraro C, Quemeneur L, Fournel S, Prigent AF, Revillard JP, Bonnefoy-Berard N. The topoisomerase inhibitors camptothecin and etoposide induce a CD95-independent apoptosis of activated peripheral lymphocytes. *Cell Death Differ.* 7(2), 197–206 (2000).
22. Ogitani Y, Abe Y, Iguchi T et al. Wide application of a novel topoisomerase I inhibitor-based drug conjugation technology. *Bioorg. Med. Chem. Lett.* 26(20), 5069–5072 (2016).
23. Tamura K, Tsurutani J, Takahashi S et al. Trastuzumab deruxtecan (DS-8201a) in patients with advanced HER2-positive breast cancer previously treated with trastuzumab emtansine: a dose-expansion, phase 1 study. *Lancet Oncol.* 20(6), 816–826 (2019).
    • **First report of preliminary safety and efficacy of Enhertu in patients with advanced HER2-positive breast cancer.**